Results in Physics 50 (2023) 106565

Contents lists available at ScienceDirect

Results in Physics

journal homepage: www.elsevier.com/locate/rinp

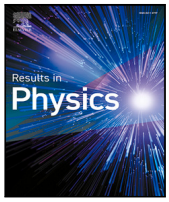

Enhanced quantum teleportation using multi-qubit logical states

Dai-Gyoung Kim [a], Arfan Anjum [b], Muhammad Asif Farooq [c], Asif Mushtaq [d,*], Zahid Hussain Shamsi [b]

[a] Department of Mathematical Data Science, Hanyang University (ERICA), Ansan, 15588, Republic of Korea
[b] Department of Mathematics, University of the Punjab, Lahore 54590, Pakistan
[c] School of Natural Sciences, National University of Sciences and Technology (NUST), Islamabad 44000, Pakistan
[d] Fakultet for lærerutd., kunst og kultur, Realfag, Nord universitet, 8049, Norway

ARTICLE INFO

Keywords:
Quantum teleportation
Logical states
Quantum error correction
Quantum entanglement
Quantum internet

ABSTRACT

In this paper, an innovative approach is suggested for quantum teleportation of multi-qubit physical state into an error correctable multi-qubit logical state. For this purpose, an efficient quantum error correction scheme is applied to detect and correct one bit flip and/or phase flip error in the teleported logical state. In addition, the proposed mechanism is substantiated by teleporting an eight-qubit physical state via four-qubit cluster state which involves three-qubit logical states as a quantum channel. The proposed scheme may be physically realized in the future fault tolerant quantum technologies.

Introduction

Quantum teleportation (QT) emerged as a fascinating manifestation of quantum information theory which has been physically realized even for very large distances. For instance, ground-to-satellite quantum teleportation has been successfully demonstrated quite recently [1]. Theoretical framework for QT was pioneered in 1993 by Bennett et al. [2] using an EPR channel [3]. Later on, the theoretical prediction was experimentally realized by two independent research groups [4,5]. Since then quantum teleportation has received great attention of the researchers who had contributed significant advancements in this area. Recent advancements include the implementation of quantum teleportation across the world using various technologies such as trapped atoms, photonic qubits, spin–orbital qubits and atomic ensembles [6–9]. In contrast to these discrete cases of teleportation, continuous variable approaches have also been envisaged for quantum teleportation [10,11]. For a comprehensive review of the recent advancements in quantum teleportation, the readers are referred to [12]. On theoretical horizon, several attempts have been made to investigate quantum teleportation at larger scale. For instance, Li et al. [13] suggested probabilistic teleportation mechanism in n dimensions. Bae et al. [14] exploited anti-symmetric property of quantum states and theoretically established that the such type of teleportation transmits significantly higher amount of information as compared to its symmetric counterpart. Zheng [15] came up with a nearly perfect teleportation through a mixture of entangled states with the aid of an ancillary particle.

More recently, multi-qubit teleportation using multi-qubit quantum channels has attracted the attention of the researchers [16–28]. In this regard, Shao [16] suggested that a two-qubit entangled state can be successfully transmitted from one place to another through four-qubit cluster states. In another attempt, Nie et al. [17] suggested the teleportation four-qubit states via six-qubit cluster states. Yang et al. [18] proposed a multi-qubit, bi-directional QT in the presence of noise. Quite recently, Zheng et al. [19] presented QT of seven-qubit state via entangled pair of four qubits.

The above mentioned multi-qubit teleportation strategies are resource efficient since these strategies use fewer qubits to teleport higher number of qubits. However, in operational sense, these strategies are susceptible to errors because these schemes employ the quantum channels which are comprised of physical qubits only. It is well known fact that these physical qubits are sensitive to various types of noise due to the interaction with the environment [29] and can induce various errors. In addition, the induced errors may propagate through the quantum circuits due to the imperfections in quantum gates used to construct these quantum circuits. Keeping in view these limitations, an enhanced quantum teleportation framework is suggested which can not only detect and correct quantum errors but can also prevent error propagation in a resource efficient way. The key feature of the proposed mechanism is to harness error resilient multi-qubit teleportation by employing multi-qubit logical states as a quantum resource. More precisely, an entangled four-qubit state is considered as quantum resource

* Corresponding author.
E-mail addresses: dgkim@hanyang.ac.kr (D.-G. Kim), asif.farooq@sns.nust.edu.pk (M.A. Farooq), asif.mushtaq@nord.no (A. Mushtaq), zahid.math@pu.edu.pk (Z.H. Shamsi).

https://doi.org/10.1016/j.rinp.2023.106565
Received 20 March 2023; Received in revised form 29 April 2023; Accepted 18 May 2023
Available online 23 May 2023

Table 1
The stabilizer formalism using the eight-qubit scheme.

$\mathscr{M}_1$	δ_x	δ_x	δ_x	δ_x	δ_x	δ_x	δ_x	δ_x
$\mathscr{M}_2$	δ_z	δ_z	δ_z	δ_z	δ_z	δ_z	δ_z	δ_z
$\mathscr{M}_3$	**I**	δ_x	**I**	δ_x	δ_y	δ_z	δ_y	δ_z
$\mathscr{M}_4$	**I**	δ_x	δ_z	δ_y	**I**	δ_x	δ_z	δ_y
$\mathscr{M}_5$	**I**	δ_y	δ_x	δ_z	δ_x	δ_z	**I**	δ_y
$\mathscr{X}_1$	δ_x	δ_x	**I**	**I**	**I**	δ_z	**I**	δ_z
$\mathscr{X}_2$	δ_x	**I**	δ_x	δ_z	**I**	**I**	δ_z	**I**
$\mathscr{X}_3$	δ_x	**I**	**I**	δ_z	δ_x	δ_z	**I**	**I**
$\mathscr{Z}_1$	**I**	δ_z	**I**	δ_z	**I**	δ_z	**I**	δ_z
$\mathscr{Z}_2$	**I**	**I**	δ_z	δ_z	**I**	**I**	δ_z	δ_z
$\mathscr{Z}_3$	**I**	**I**	**I**	**I**	δ_z	δ_z	δ_z	δ_z

between the sender (Alice) and the receiver (Bob), where Alice holds a physical qubit as usual. However, Bob possesses three-qubit logical state encoded via a suitable quantum error correction code (QECC). The proposed mechanism is in stark contrast to the above mentioned multi-qubit teleportation strategies where the quantum channels involve only physical (un-encoded) multi-qubit states on both Alice and Bob's sides. The proposed strategy ensures the detection and correction of certain types of one bit errors through a rigorous non-degenerate stabilizer formalism [29–33]. In addition, this formalism also prevents further propagation of the errors through the quantum circuits owing to transversal nature of the logical gates. Furthermore, the suggested mechanism is applied to teleport an unknown eight-qubit physical state in a resource efficient way.

The organization of the paper is outlined in the following. The quantum error correction (QEC) mechanism employed in the proposed quantum teleportation framework is described in Section "Quantum error correction and logical quantum states". The proposed quantum teleportation framework and its distinct features are entailed in Section "Methodology". The capability of the proposed framework to withstand security attacks is depicted in Section "Security evaluation". Lastly, the conclusions are drawn in Section "Conclusion".

Quantum error correction and logical quantum states

Prior to describing the proposed framework for multi-qubit physical state teleportation into multi-qubit logical states, the necessary details are provided for the multi-qubit logical states and the corresponding quantum error correction codes considered in this paper.

With the increase in the size of quantum circuit, imperfections in the physical realization of quantum gates induce errors which in turn may produce undesired and inconsistent results [34]. Depending upon the nature of errors, various quantum error correction (QEC) schemes have been proposed to identify and amend those errors accordingly [31–33,35]. The key principle of any QEC schemes is to design logical qubits (encoded states) and the stabilizers that preserve the invariance of those logical states which can withstand those errors.

Encoded state preparation

In this paper, three qubit encoding scheme using eight qubits, $[[8,3,3]]$, is considered [31,33] which is shown in Table 1. Here, $\{\mathscr{M}_i\}_{i=1}^{5}$ generates the abelian subgroup S of the unitary Pauli group G_8. The subgroup S is called stabilizer and it preserves the invariance of the three-qubit logical code $|\varphi\rangle$. That is, we can define the code space $T = \{|\varphi\rangle \text{ s.t. } \mathscr{M}|\varphi\rangle = |\varphi\rangle \ \forall \mathscr{M} \in S\}$.

The generators $\mathscr{M}_1$ through $\mathscr{M}_5$ along with $\mathscr{X}_i$ and $\mathscr{Z}_i$, $(i = 1,2,3)$, generate the normalizer group $\mathscr{N}(S)$. The group S is contained in $\mathscr{N}(S)$. The main difference between S and $\mathscr{N}(S)$ is that S is invariant under conjugation. That is, for any element $g \in G_8$, $gSg^{-1} = S$. The three-qubit logical states are obtained by using the elements of S and $\mathscr{N}(S)$ as follows [29,31]

$$|\overline{000}\rangle = \prod_{i=1}^{5}\left(\mathbb{I} + \mathscr{M}_i\right)|000000000\rangle = \sum_{\mathscr{M}\in S}\mathscr{M}|000000000\rangle, \tag{1}$$

$$|\overline{010}\rangle = \mathscr{X}_2|\overline{000}\rangle, \tag{2}$$

$$|\overline{101}\rangle = \mathscr{X}_1\mathscr{X}_3|\overline{000}\rangle, \tag{3}$$

$$|\overline{111}\rangle = \mathscr{X}_1\mathscr{X}_2\mathscr{X}_3|\overline{000}\rangle. \tag{4}$$

The logical states $|\overline{000}\rangle$ and $|\overline{111}\rangle$ are explicitly described as

$$\begin{aligned}|\overline{000}\rangle = \frac{1}{4}(&|00000000\rangle - |00001111\rangle + |00110011\rangle + |00111100\rangle\\ &+ |01010101\rangle - |01011010\rangle - |01100110\rangle\\ &- |01101001\rangle + |11111111\rangle - |11110000\rangle\\ &+ |11001100\rangle + |11000011\rangle\\ &+ |10101010\rangle - |10100101\rangle\\ &- |10011001\rangle - |10010110\rangle),\end{aligned} \tag{5}$$

$$\begin{aligned}|\overline{111}\rangle = \frac{1}{4}(&|00010111\rangle - |00011000\rangle + |00100100\rangle + |00101011\rangle\\ &+ |01000010\rangle - |01001101\rangle - |01110001\rangle\\ &- |01111110\rangle + |10000001\rangle - |10001110\rangle\\ &+ |10110010\rangle + |10111101\rangle\\ &+ |11010100\rangle - |11011011\rangle\\ &- |11100111\rangle - |11101000\rangle).\end{aligned} \tag{6}$$

Since the generators, $\mathscr{M}_i$, commute with each other and the encoding scheme is non-degenerate, these generators have common eigenstates. Hence, the input state $|0\rangle^{\otimes 8}$ is projected into an eigenstate of each of the $\mathscr{M}$ stabilizers defined in Table 1 using five ancillary qubits. The encoding quantum circuit and the encoded states are shown in Fig. 1 and Fig. 2, respectively.

Error detection and correction

As described earlier, the abelian subgroup S preserves the invariance of the three-qubit logical code $|\varphi\rangle$. That is, S generates the code space $T = \{|\varphi\rangle \text{ s.t. } \mathscr{M}|\varphi\rangle = |\varphi\rangle \ \forall \mathscr{M} \in S\}$. Since all the generators $\mathscr{M}_i$ commute with each other, the task of detecting any error E is determined by evaluating anti-commutation of E with any of these generators. Mathematically, it can be explained as follows. Suppose E anti-commutes with $\mathscr{M}_3$ i.e., $\mathscr{M}_3E = -E\mathscr{M}_3$. Then, for any $|\varphi\rangle \in T$ and the error E

$$\mathscr{M}_3E|\varphi\rangle = -E\underbrace{\mathscr{M}_3|\varphi\rangle}_{\mathscr{M}_3|\varphi\rangle=|\varphi\rangle} = -E|\varphi\rangle. \tag{7}$$

Note that $E|\varphi\rangle$ represents an erroneous state since it is not a valid code i.e., $E|\varphi\rangle \notin T$. However, the location of error is not yet completely determined. In order to find the location of error, the encoding scheme is represented in symplectic notation [33] as

$$\mathbb{M} = \left(\begin{array}{cccccccc|cccccccc}
0&0&0&0&0&0&0&0&1&1&1&1&1&1&1&1\\
1&1&1&1&1&1&1&1&0&0&0&0&0&0&0&0\\
1&0&1&0&1&0&1&0&0&1&1&0&0&1&1&0\\
0&1&1&0&0&1&1&0&0&0&0&1&1&1&1&0\\
0&0&0&1&1&1&1&0&1&1&0&0&1&1&0&0
\end{array}\right), \tag{8}$$

where the non-zero entries correspond to δ_z and δ_x or I in the left and right partitions of the matrix, respectively. This representation offers a relatively simpler way of analyzing the error detection and correction mechanism. Note that the encoding scheme is non-degenerate since

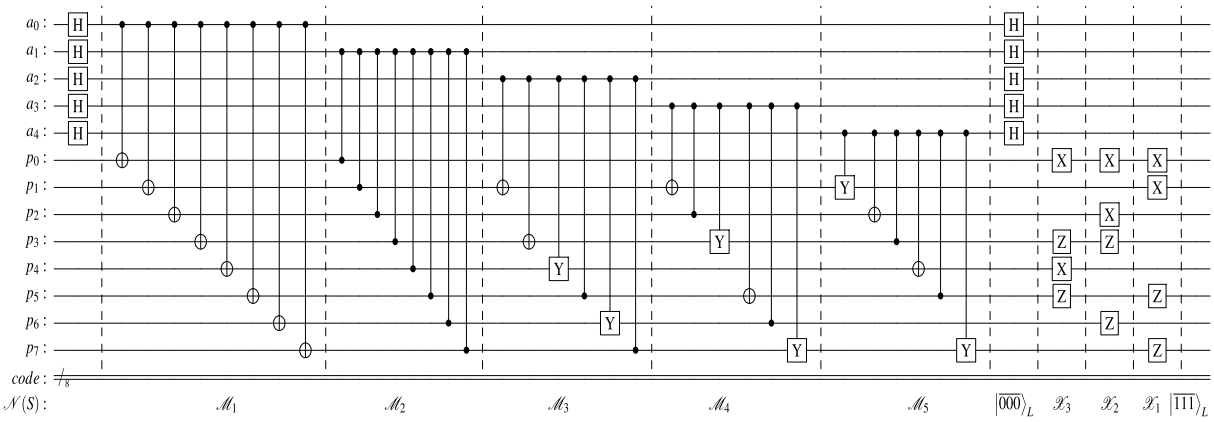

Fig. 1. The quantum circuit to prepare three qubit encoded states $|\overline{000}\rangle_L$ and $|\overline{111}\rangle_L$ from the eight qubit physical qubits.

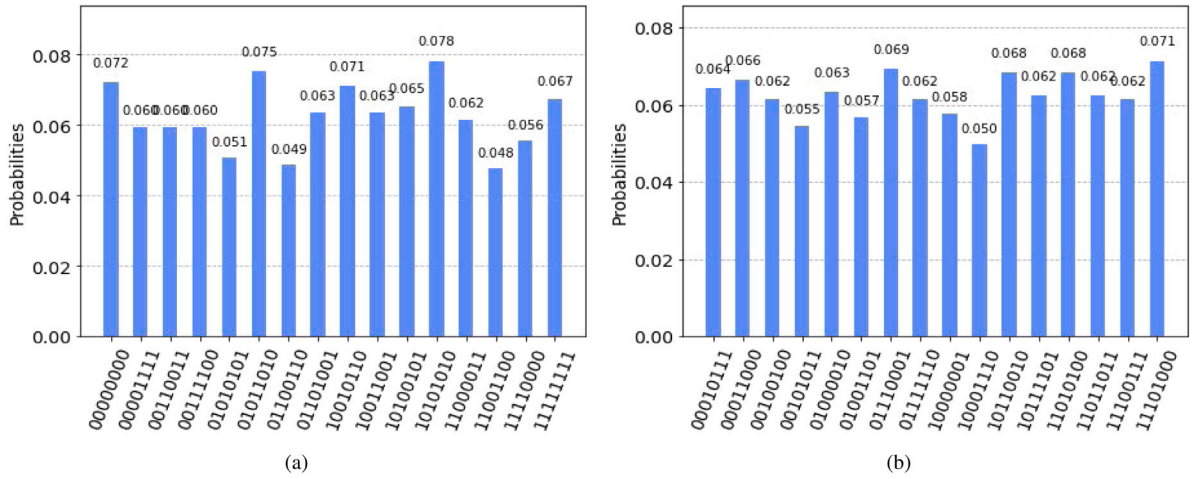

Fig. 2. The left and right side figures represent the three qubit logical states $|\overline{000}\rangle_L$ and $|\overline{111}\rangle_L$, respectively, prepared by the circuit shown in Fig. 1.

the rows of $\mathbb{M}$ are pairwise orthogonal. It implies that the encoding scheme assigns a unique code for each one bit error. Furthermore, each column may be viewed as *error syndrome* for a single qubit error. The left and right sides of $\mathbb{M}$ can diagnose at most one single bit flip error or phase flip error, respectively [31]. In the following, the error detection process is briefly explained for a bit flip and phase flip errors.

Bit-flip error detection

Suppose the initial encoded state be given by

$$\begin{aligned}|\phi\rangle = \frac{1}{4}(&|00000000\rangle - |00001111\rangle + |00110011\rangle + |00111100\rangle\\ &+|01010101\rangle - |01011010\rangle - |01100110\rangle\\ &-|01101001\rangle + |11111111\rangle - |11110000\rangle + |11001100\rangle\\ &+|11000011\rangle + |10101010\rangle - |10100101\rangle\\ &-|10011001\rangle - |10010110\rangle).\end{aligned} \tag{9}$$

Further assume that a bit flip error, E_x, occurs on any of the eight physical qubits yielding the resultant state

$$\begin{aligned}E_x|\phi\rangle = \frac{1}{4}(&|01000000\rangle - |01001111\rangle + |01110011\rangle + |01111100\rangle\\ &+|00010101\rangle - |00011010\rangle - |00100110\rangle\\ &-|00101001\rangle + |10111111\rangle - |10110000\rangle + |10001100\rangle\\ &+|10000011\rangle + |11101010\rangle - |11100101\rangle\\ &-|11011001\rangle - |11010110\rangle).\end{aligned} \tag{10}$$

To detect the location of the error, each of the generators, $\mathscr{M}_i$, is applied to $E_x|\phi\rangle$. The results of these operations are shown below

$$\begin{aligned}\mathscr{M}_1 E_x|\phi\rangle &= E_x|\phi\rangle,\\ \mathscr{M}_2 E_x|\phi\rangle &= -E_x|\phi\rangle,\\ \mathscr{M}_3 E_x|\phi\rangle &= E_x|\phi\rangle,\\ \mathscr{M}_4 E_x|\phi\rangle &= -E_x|\phi\rangle,\\ \mathscr{M}_5 E_x|\phi\rangle &= E_x|\phi\rangle.\end{aligned} \tag{11}$$

Note that, negative sign appears for $\mathscr{M}_2$ and $\mathscr{M}_4$. It can further be noticed that the second column in Table 2 indicates non-zero entries only for $\mathscr{M}_2$ and $\mathscr{M}_4$. Therefore, these results reflect that bit flip error has occurred on the second qubit location. This result is also shown in Fig. 3(a) using the same quantum circuit drawn in Fig. 1 with the erroneous state (10) as an input. Consequently, the corresponding correction operation $\mathbf{I}\otimes\delta_x\otimes\mathbf{I}^{\otimes 6}$ on the state (10) restores the original state (9).

In essence, the detection procedure provides a unique combination of the generators which anti-commutes with the given E_x. This combination matches with a unique column of Table 2. The index of the column returns the location of E_x error which can then be easily corrected as mentioned above.

Phase flip error detection

Starting with the same encoded state (9), suppose the phase flip error E_z occurs on any of the eight qubits yielding the state

$$E_z|\phi\rangle = \frac{1}{4}(|00000000\rangle + |00001111\rangle - |00110011\rangle + |00111100\rangle$$

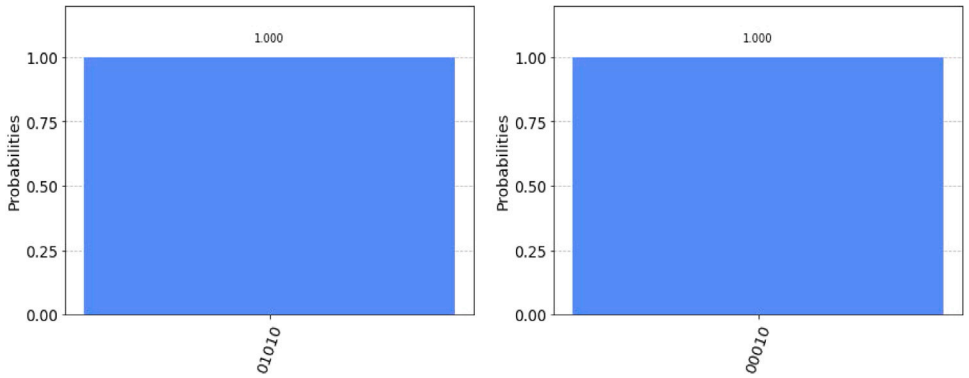

Fig. 3. The left and right figures represent the syndrome extraction for bit flip error on the second and eighth locations, respectively, as predicted in Table 2. The syndrome extraction is implemented using the same circuit shown in Fig. 1 with the erroneous states as inputs.

Table 2
Detection of bit flip error (the left partition of $\mathbb{M}$).

	δ_{z1}	δ_{z2}	δ_{z3}	δ_{z4}	δ_{z5}	δ_{z6}	δ_{z7}	δ_{z8}
$\mathscr{M}_1$	0	0	0	0	0	0	0	0
$\mathscr{M}_2$	1	1	1	1	1	1	1	1
$\mathscr{M}_3$	1	0	1	0	1	0	1	0
$\mathscr{M}_4$	0	1	1	0	0	1	1	0
$\mathscr{M}_5$	0	0	0	1	1	1	1	0

Table 3
Detection of the phase flip error (the right partition of $\mathbb{M}$).

	δ_{x1}	δ_{x2}	δ_{x3}	δ_{x4}	δ_{x5}	δ_{x6}	δ_{x7}	δ_{x8}
$\mathscr{M}_1$	1	1	1	1	1	1	1	1
$\mathscr{M}_2$	0	0	0	0	0	0	0	0
$\mathscr{M}_3$	0	1	1	0	0	1	1	0
$\mathscr{M}_4$	0	0	0	1	1	1	1	0
$\mathscr{M}_5$	1	1	0	0	1	1	0	0

$$
\begin{aligned}
&+|01010101\rangle - |01011010\rangle - |01100110\rangle \\
&+|01101001\rangle - |11111111\rangle - |11110000\rangle + |11001100\rangle \\
&- |11000011\rangle + |10101010\rangle + |10100101\rangle \\
&+ |10011001\rangle - |10010110\rangle). \qquad (12)
\end{aligned}
$$

Proceeding in the similar fashion, each of the generators, $\mathscr{M}_i$, is applied to the above encoded state. The corresponding results are given as

$$
\begin{aligned}
\mathscr{M}_1 E_z|\phi\rangle &= -E_z|\phi\rangle, \\
\mathscr{M}_2 E_z|\phi\rangle &= E_z|\phi\rangle, \\
\mathscr{M}_3 E_z|\phi\rangle &= E_z|\phi\rangle, \\
\mathscr{M}_4 E_z|\phi\rangle &= E_z|\phi\rangle, \\
\mathscr{M}_5 E_z|\phi\rangle &= E_z|\phi\rangle. \qquad (13)
\end{aligned}
$$

In this case, the negative sign appears only for $\mathscr{M}_1$. By looking up Table 3, it turned out that only the last column involves non-zero entry against $\mathscr{M}_1$ while it has zero entries for the rest of the generators as shown in Fig. 4(a). Therefore, it can be easily inferred that the phase error has occurred on the eighth location. Accordingly, the error can be corrected by applying the operator $\mathbf{I}^{\otimes 7} \otimes \delta_z$ to the state (12).

In the similar fashion, the simultaneous phase and bit flip error on any qubit can be detected and correcting using the Table 4. It is also important to note that the columns of this table are obtained by just adding the corresponding columns given in Tables 2 and 3. This is due the fact that δ_{y_i} at location i anti-commutes with both δ_x and δ_z at the corresponding location in their respective tables (see Fig. 5).

Table 4
Detection of simultaneous bit and phase flip errors.

	δ_{y1}	δ_{y2}	δ_{y3}	δ_{y4}	δ_{y5}	δ_{y6}	δ_{y7}	δ_{y8}
$\mathscr{M}_1$	1	1	1	1	1	1	1	1
$\mathscr{M}_2$	1	1	1	1	1	1	1	1
$\mathscr{M}_3$	1	1	0	0	1	1	0	0
$\mathscr{M}_4$	0	1	1	1	1	0	0	0
$\mathscr{M}_5$	1	1	0	1	0	0	1	0

Methodology

Proposed quantum teleportation

The suggested mechanism is inspired by a recent physical realization of teleporting single qubit physical state into a logical state where Alice and Bob jointly possess an entangled state of one physical qubit owned by Alice and one logical state owned by Bob [36]. However, the proposed quantum teleportation significantly differs from the said approach in the following two ways. Firstly, the proposed mechanism used four qubit entangled state shared between Alice and Bob, allowing multi-qubit physical state teleportation into multi-qubit logical state. Secondly, the suggested encoding scheme utilized an eight qubit non-degenerate code $[[8, 3, 3]]$ to construct three qubit logical states [33] whereas $[[9, 1, 3]]$ code is used in [36] which employs nine physical qubits to design one logical qubit [30,37].

In what follows, the proposed teleportation scheme of three-qubit physical state into a three qubit logical state is explained succeeded by an extension of the proposed mechanism for an eight qubit physical state teleportation into three qubit logical space. For this purpose, the following cluster state possessed by the sender, Alice, and the receiver, Bob, is considered

$$|C\rangle_{\overline{1234}} = \frac{1}{2}(|\overline{0000}\rangle + |\overline{0101}\rangle + |\overline{1010}\rangle - |\overline{1111}\rangle)_{1234}, \qquad (14)$$

where the physical qubit $|c_1\rangle$ is possessed by Alice and the remaining logical qubits $|\overline{c_2c_3c_4}\rangle$ are possessed by Bob. The unknown three qubit physical state to be teleported is given as

$$|\psi\rangle_{abc} = \lambda|000\rangle + \mu|001\rangle + \nu|110\rangle + \omega|111\rangle, \qquad (15)$$

where it is customary to mention the normalization constraint $|\lambda|^2 + |\mu|^2 + |\nu|^2 + |\omega|^2 = 1$. The joint state of the three-qubit physical state and quantum channel (QC) is then given by

$$|\eta\rangle_{abc1234} = |\psi\rangle_{abc} \otimes |C\rangle_{\overline{1234}}. \qquad (16)$$

In order to implement the proposed teleportation scheme, the first four qubits, indexed by $abc1$, of the combined state (16) are described as a

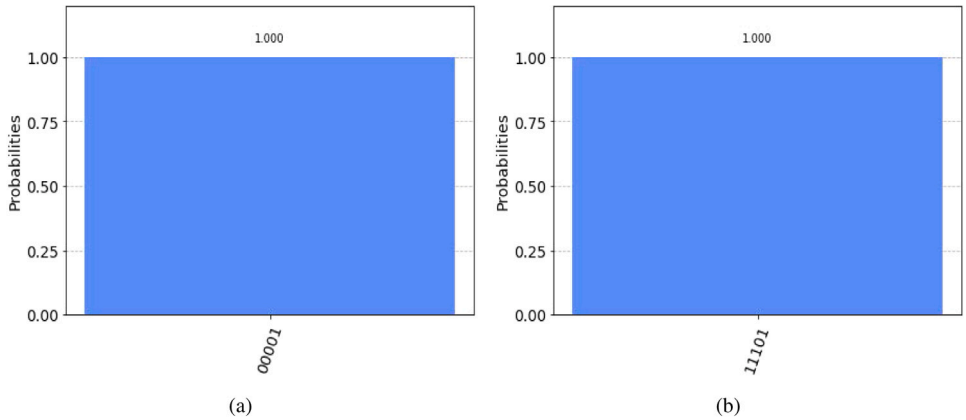

Fig. 4. The left and right figures represent the syndrome extraction for the phase flip error on the eighth and sixth locations, respectively, as predicted in Table 3. The syndrome extraction is implemented using the same circuit shown in Fig. 1 with the erroneous states as inputs.

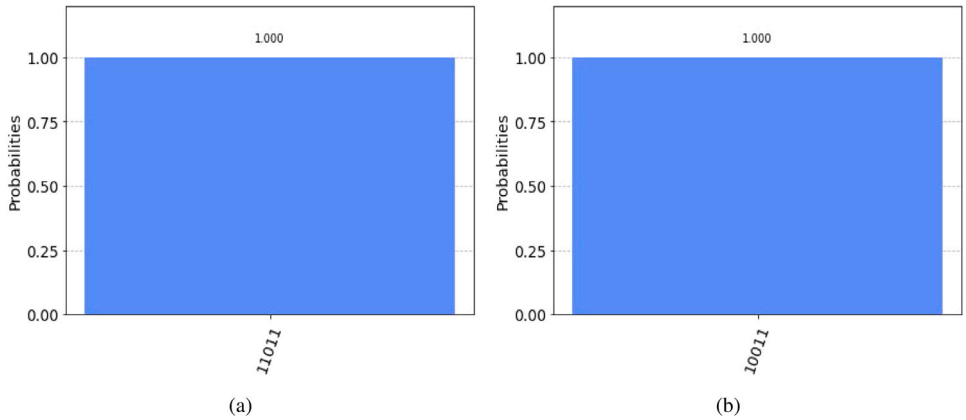

Fig. 5. The left and right figures represent the syndrome extraction for simultaneous bit and phase flip error on the fourth and seventh locations, respectively, as predicted in Table 4. The syndrome extraction is implemented using the same circuit shown in Fig. 1 with the erroneous states as inputs.

superposition of the following mutually orthogonal basis $\{|\zeta^i\rangle_{abc1}\}_{i=1}^{16}$

$$|\zeta^1\rangle = \frac{1}{2}[|0000\rangle + |0101\rangle + |1010\rangle + |1111\rangle]_{abc1},$$
$$|\zeta^2\rangle = \frac{1}{2}[|0000\rangle - |0101\rangle + |1010\rangle - |1111\rangle]_{abc1},$$
$$|\zeta^3\rangle = \frac{1}{2}[|0000\rangle + |0101\rangle - |1010\rangle - |1111\rangle]_{abc1,}$$
$$|\zeta^4\rangle = \frac{1}{2}[|0000\rangle - |0101\rangle - |1010\rangle + |1111\rangle]_{abc1},$$
$$|\zeta^5\rangle = \frac{1}{2}[|0001\rangle + |0100\rangle + |1011\rangle + |1111\rangle]_{abc1},$$
$$|\zeta^6\rangle = \frac{1}{2}[|0001\rangle - |0100\rangle + |1011\rangle - |1111\rangle]_{abc1},$$
$$|\zeta^7\rangle = \frac{1}{2}[|0001\rangle + |0100\rangle - |1011\rangle - |1111\rangle]_{abc1},$$
$$|\zeta^8\rangle = \frac{1}{2}[|0001\rangle - |0100\rangle - |1011\rangle + |1111\rangle]_{abc1},$$
$$|\zeta^9\rangle = \frac{1}{2}[|0010\rangle + |0111\rangle + |1000\rangle + |1101\rangle]_{abc1},$$
$$|\zeta^{10}\rangle = \frac{1}{2}[|0010\rangle - |0111\rangle + |1000\rangle - |1101\rangle]_{abc1},$$
$$|\zeta^{11}\rangle = \frac{1}{2}[|0010\rangle + |0111\rangle - |1000\rangle - |1101\rangle]_{abc1},$$
$$|\zeta^{12}\rangle = \frac{1}{2}[|0010\rangle - |0111\rangle - |1000\rangle + |1101\rangle]_{abc1},$$
$$|\zeta^{13}\rangle = \frac{1}{2}[|0011\rangle + |0110\rangle + |1001\rangle + |1100\rangle]_{abc1},$$
$$|\zeta^{14}\rangle = \frac{1}{2}[|0011\rangle - |0110\rangle + |1001\rangle - |1100\rangle]_{abc1},$$
$$|\zeta^{15}\rangle = \frac{1}{2}[|0011\rangle + |0110\rangle - |1001\rangle - |1100\rangle]_{abc1},$$
$$|\zeta^{16}\rangle = \frac{1}{2}[|0011\rangle + |0110\rangle + |1001\rangle + |1100\rangle]_{abc1}. \quad (17)$$

Consequently, the combined state $|\eta\rangle_{abc1234}$ given in (16) can now be re-written in the above basis as

$$\begin{aligned}
|\eta\rangle_{abc1234} = \frac{1}{4}\Big[& |\zeta^1\rangle(\lambda|\overline{000}\rangle + \mu|\overline{010}\rangle + \nu|\overline{101}\rangle + \omega|\overline{111}\rangle)_{234} \\
& + |\zeta^2\rangle(\lambda|\overline{000}\rangle - \mu|\overline{010}\rangle + \nu|\overline{101}\rangle - \omega|\overline{111}\rangle)_{234} \\
& + |\zeta^3\rangle(\lambda|\overline{000}\rangle + \mu|\overline{010}\rangle - \nu|\overline{101}\rangle - \omega|\overline{111}\rangle)_{234} \\
& + |\zeta^4\rangle(\lambda|\overline{000}\rangle - \mu|\overline{010}\rangle - \nu|\overline{101}\rangle + \omega|\overline{111}\rangle)_{234} \\
& + |\zeta^5\rangle(\lambda|\overline{010}\rangle + \mu|\overline{000}\rangle + \nu|\overline{111}\rangle + \omega|\overline{101}\rangle)_{234} \\
& + |\zeta^6\rangle(\lambda|\overline{010}\rangle - \mu|\overline{000}\rangle + \nu|\overline{111}\rangle - \omega|\overline{101}\rangle)_{234} \\
& + |\zeta^7\rangle(\lambda|\overline{010}\rangle + \mu|\overline{000}\rangle - \nu|\overline{111}\rangle - \omega|\overline{101}\rangle)_{234} \\
& + |\zeta^8\rangle(\lambda|\overline{010}\rangle - \mu|\overline{000}\rangle - \nu|\overline{111}\rangle + \omega|\overline{101}\rangle)_{234} \\
& + |\zeta^9\rangle(\lambda|\overline{101}\rangle + \mu|\overline{111}\rangle + \nu|\overline{000}\rangle + \omega|\overline{010}\rangle)_{234} \\
& + |\zeta^{10}\rangle(\lambda|\overline{101}\rangle - \mu|\overline{111}\rangle + \nu|\overline{000}\rangle - \omega|\overline{010}\rangle)_{234} \\
& + |\zeta^{11}\rangle(\lambda|\overline{101}\rangle + \mu|\overline{111}\rangle - \nu|\overline{000}\rangle - \omega|\overline{010}\rangle)_{234} \\
& + |\zeta^{12}\rangle(\lambda|\overline{101}\rangle - \mu|\overline{111}\rangle - \nu|\overline{000}\rangle + \omega|\overline{010}\rangle)_{234} \\
& + |\zeta^{13}\rangle(\lambda|\overline{111}\rangle + \mu|\overline{101}\rangle + \nu|\overline{010}\rangle + \omega|\overline{000}\rangle)_{234} \\
& + |\zeta^{14}\rangle(\lambda|\overline{111}\rangle - \mu|\overline{101}\rangle + \nu|\overline{010}\rangle - \omega|\overline{000}\rangle)_{234} \\
& + |\zeta^{15}\rangle(\lambda|\overline{111}\rangle + \mu|\overline{101}\rangle - \nu|\overline{010}\rangle - \omega|\overline{000}\rangle)_{234} \\
& + |\zeta^{16}\rangle(\lambda|\overline{111}\rangle - \mu|\overline{101}\rangle - \nu|\overline{010}\rangle + \omega|\overline{000}\rangle)_{234}\Big]. \quad (18)
\end{aligned}$$

Now, Alice performs the measurement on her side by utilizing the basis defined by (17). The measurement results in the collapse of the superimposed state (18) into one of the basis states $|\zeta^i\rangle_{abc1}$ for

Table 5
The logical qubits obtained by Bob after measurement by Alice.

Alice's result	Classical information	Bob's state	Bob's operation
$\|\zeta^1\rangle$	0000	$\lambda\|\overline{000}\rangle + \mu\|\overline{010}\rangle + \nu\|\overline{101}\rangle + \omega\|\overline{111}\rangle$	$I^{\otimes 8}$
$\|\zeta^2\rangle$	0001	$\lambda\|\overline{000}\rangle - \mu\|\overline{010}\rangle + \nu\|\overline{101}\rangle - \omega\|\overline{111}\rangle$	$\mathscr{Z}_2$
$\|\zeta^3\rangle$	0010	$\lambda\|\overline{000}\rangle + \mu\|\overline{010}\rangle - \nu\|\overline{101}\rangle - \omega\|\overline{111}\rangle$	$\mathscr{Z}_3$
$\|\zeta^4\rangle$	0011	$\lambda\|\overline{000}\rangle - \mu\|\overline{010}\rangle - \nu\|\overline{101}\rangle + \omega\|\overline{111}\rangle$	$\mathscr{Z}_1\mathscr{Z}_2$
$\|\zeta^5\rangle$	0100	$\lambda\|\overline{010}\rangle + \mu\|\overline{000}\rangle + \nu\|\overline{111}\rangle + \omega\|\overline{101}\rangle$	$\mathscr{X}_2$
$\|\zeta^6\rangle$	0101	$\lambda\|\overline{010}\rangle - \mu\|\overline{000}\rangle + \nu\|\overline{111}\rangle - \omega\|\overline{101}\rangle$	$\mathscr{Z}_2\mathscr{X}_2$
$\|\zeta^7\rangle$	0110	$\lambda\|\overline{010}\rangle + \mu\|\overline{000}\rangle - \nu\|\overline{111}\rangle - \omega\|\overline{101}\rangle$	$\mathscr{X}_2\mathscr{Z}_3$
$\|\zeta^8\rangle$	0111	$\lambda\|\overline{010}\rangle - \mu\|\overline{000}\rangle - \nu\|\overline{111}\rangle + \omega\|\overline{101}\rangle$	$\mathscr{Z}_2\mathscr{X}_2\mathscr{Z}_3$
$\|\zeta^9\rangle$	1000	$\lambda\|\overline{101}\rangle + \mu\|\overline{111}\rangle + \nu\|\overline{000}\rangle + \omega\|\overline{010}\rangle$	$\mathscr{X}_1\mathscr{X}_3$
$\|\zeta^{10}\rangle$	1001	$\lambda\|\overline{101}\rangle - \mu\|\overline{111}\rangle + \nu\|\overline{000}\rangle - \omega\|\overline{010}\rangle$	$\mathscr{X}_1\mathscr{Z}_2\mathscr{X}_3$
$\|\zeta^{11}\rangle$	1010	$\lambda\|\overline{101}\rangle + \mu\|\overline{111}\rangle - \nu\|\overline{000}\rangle - \omega\|\overline{010}\rangle$	$\mathscr{X}_1\mathscr{Z}_3\mathscr{X}_3$
$\|\zeta^{12}\rangle$	1011	$\lambda\|\overline{101}\rangle - \mu\|\overline{111}\rangle - \nu\|\overline{000}\rangle + \omega\|\overline{010}\rangle$	$\mathscr{Z}_1\mathscr{X}_1\mathscr{Z}_2\mathscr{X}_3$
$\|\zeta^{13}\rangle$	1100	$\lambda\|\overline{111}\rangle + \mu\|\overline{101}\rangle + \nu\|\overline{010}\rangle + \omega\|\overline{000}\rangle$	$\mathscr{X}_1\mathscr{X}_2\mathscr{X}_3$
$\|\zeta^{14}\rangle$	1101	$\lambda\|\overline{111}\rangle - \mu\|\overline{101}\rangle + \nu\|\overline{010}\rangle - \omega\|\overline{000}\rangle$	$\mathscr{X}_1\mathscr{Z}_2\mathscr{X}_2\mathscr{X}_3$
$\|\zeta^{15}\rangle$	1110	$\lambda\|\overline{111}\rangle + \mu\|\overline{101}\rangle - \nu\|\overline{010}\rangle - \omega\|\overline{000}\rangle$	$\mathscr{X}_1\mathscr{X}_2\mathscr{Z}_3\mathscr{X}_3$
$\|\zeta^{16}\rangle$	1111	$\lambda\|\overline{111}\rangle - \mu\|\overline{101}\rangle - \nu\|\overline{010}\rangle + \omega\|\overline{000}\rangle$	$\mathscr{Z}_1\mathscr{X}_1\mathscr{Z}_2\mathscr{X}_2\mathscr{X}_3$

some i. Subsequently, Alice communicates measurement results to Bob through classical channel. As a result of the measurement, Bob's state has been transformed into one of the sixteen three qubit logical states provided in Table 5. It is worth noticing that the proposed teleportation scheme differs from the conventional teleportation mechanisms where the unknown physical qubits are teleported into the physical qubits. Here, the physical qubit are teleported into the logical qubits using the quantum channel involving the entanglement between the one physical and three logical qubits.

In order to recover the teleported state (the three qubit logical state) Bob performs the encoded (logical) unitary operations $\mathscr{X}_i$'s and $\mathscr{Z}_i$'s defined in Table 1. These logical operations acting on Bob's state are shown in the last column of Table 5. Since the logical operators $\mathscr{X}$ and $\mathscr{Z}$ are the elements of the normalizer subgroup $\mathscr{N}(S)$, these operators just transform the logical state (element of the code space T) into some other logical state in T. More precisely, these transformations ensure that the encoded states must remain within the code space T. It is also emphasized that these logical operations recover the original encoded state in a fault tolerant fashion. It implies that the operations directly operate on the logical states without any limitation of decoding and then re-encoding process. Furthermore, these logical operations are transversal gates and act independently on each physical qubit in the logical state. This mechanism ensures that errors do not propagate during the computation. Finally, Bob can recover the original three qubit physical state just by taking adjoint of the encoding operation since the stabilizer group S is unitary.

Noise analysis

To examine the efficiency of the proposed QEC scheme for quantum teleportation, we estimate and compare the fidelities of physical (un-encoded) and logical (encoded) qubits in the presence of coherent Pauli noise [30,31,33]. Consider the single qubit coherent noise operator, $E = exp(i\epsilon\delta_x)$ with the assumption that each of the physical qubit is susceptible to this noise where $\epsilon \ll 1$. Then, the action of E on the logical state $|\phi\rangle_L$ yields

$$\begin{aligned}|\phi\rangle_E &= E^{\otimes 8}|\phi\rangle_L = \left(\cos\epsilon\mathbf{I} + i\sin\epsilon\boldsymbol{\delta_x}\right)^{\otimes 8}|\phi\rangle_L, \\ &= \Big[\ \alpha_0\mathbf{I}^{\otimes 8} + \alpha_1(\delta_x\otimes\mathbf{I}^{\otimes 7} + \mathbf{I}\otimes\delta_x\otimes\mathbf{I}^{\otimes 6} \\ &\quad + \mathbf{I}^{\otimes 2}\otimes\delta_x\otimes\mathbf{I}^{\otimes 5} + \cdots + \mathbf{I}^{\otimes 7}\otimes\delta_x) \\ &\quad + \alpha_2(\delta_x^{\otimes 2}\otimes\mathbf{I}^{\otimes 6} + \delta_x\otimes\mathbf{I}\otimes\delta_x\otimes\mathbf{I}^{\otimes 5} \\ &\quad + \delta_x\otimes\mathbf{I}^{\otimes 2}\otimes\delta_x\otimes\mathbf{I}^{\otimes 4} + \cdots + \mathbf{I}^{\otimes 6}\delta_x^{\otimes 2}) \\ &\quad + \cdots + \alpha_7(\delta_x^{\otimes 7}\otimes\mathbf{I} + \delta_x^{\otimes 6}\otimes\mathbf{I}\otimes\delta_x \\ &\quad + \delta_x^{\otimes 5}\otimes\mathbf{I}\otimes\delta_x^{\otimes 2} + \cdots + \mathbf{I}\otimes\delta_x^{\otimes 7}) + \alpha_8\delta_x^{\otimes 8}\ \Big]\ |\phi\rangle_L, \end{aligned} \tag{19}$$

$$\begin{aligned}|\phi\rangle_E &= E^{\otimes 8}|\phi\rangle_L = \left(\cos\epsilon\mathbf{I} + i\sin\epsilon\boldsymbol{\delta_x}\right)^{\otimes 8}|\phi\rangle_L, \\ &= \Big[\ \alpha_0\mathbf{I}^{\otimes 8} + \alpha_1(\delta_x\otimes\mathbf{I}^{\otimes 7} + \mathbf{I}\otimes\delta_x\otimes\mathbf{I}^{\otimes 6} \\ &\quad + \mathbf{I}^{\otimes 2}\otimes\delta_x\otimes\mathbf{I}^{\otimes 5} + \cdots + \mathbf{I}^{\otimes 7}\otimes\delta_x) \\ &\quad + \alpha_2(\delta_x^{\otimes 2}\otimes\mathbf{I}^{\otimes 6} + \delta_x\otimes\mathbf{I}\otimes\delta_x\otimes\mathbf{I}^{\otimes 5} \\ &\quad + \delta_x\otimes\mathbf{I}^{\otimes 2}\otimes\delta_x\otimes\mathbf{I}^{\otimes 4} + \cdots + \mathbf{I}^{\otimes 6}\delta_x^{\otimes 2}) \\ &\quad + \cdots + \alpha_7(\delta_x^{\otimes 7}\otimes\mathbf{I} + \delta_x^{\otimes 6}\otimes\mathbf{I}\otimes\delta_x \\ &\quad + \delta_x^{\otimes 5}\otimes\mathbf{I}\otimes\delta_x^{\otimes 2} + \cdots + \mathbf{I}\otimes\delta_x^{\otimes 7}) + \alpha_8\delta_x^{\otimes 8}\ \Big]\ |\phi\rangle_L, \end{aligned} \tag{20}$$

where the coefficients α_i's,$(i = 0, 1, \ldots, 8)$ are given by

$$\begin{aligned}&\alpha_0 = \cos^8\epsilon, \quad \alpha_1 = i\cos^7\epsilon\sin^1\epsilon, \quad \alpha_2 = -\cos^6\epsilon\sin^2\epsilon, \\ &\alpha_3 = -i\cos^5\epsilon\sin^3\epsilon, \quad \alpha_4 = \cos^4\epsilon\sin^4\epsilon, \\ &\alpha_5 = i\cos^3\epsilon\sin^5\epsilon, \quad \alpha_6 = -\cos^2\epsilon\sin^6\epsilon, \\ &\alpha_7 = -i\cos^1\epsilon\sin^7\epsilon, \quad \alpha_8 = \sin^8\epsilon. \end{aligned} \tag{21}$$

Note that the coefficient α_0 corresponds to the noise free state $|\phi\rangle_L$ and the coefficient α_8 corresponds to no error detected state since $\delta_x^{\otimes 8}$ just flips each of the physical qubit in $|\phi\rangle_L$. The rest of the coefficients α_1 through α_7 represent erroneous states.

Let us first consider the action of the coherent error E_x on single physical (un-encoded) qubit $|\phi\rangle_P$ given by

$$E_x|\phi\rangle_P = \cos\epsilon|\phi\rangle_P + i\sin\epsilon\delta_x|\phi\rangle_P. \tag{22}$$

The fidelity of the un-encoded state will then be

$$\mathscr{F}_{phy} = |{}_P\langle\phi|E_x|\phi\rangle_P|^2 = \cos^2\epsilon \approx 1 - \epsilon^2. \tag{23}$$

In case of single logical (encoded) state $|\phi\rangle_L$, we evaluate two fidelities. The fidelity when no error is detected and the fidelity when an error is detected. In case of no error detection, the fidelity is given by

$$\begin{aligned}\mathscr{F}_{\text{no error found}} &= |{}_L\langle\phi|E_x^{\otimes 8}|\phi\rangle_L|^2, \\ &= \frac{|\alpha_0|^2}{|\alpha_0|^2 + |\alpha_8|^2} = \frac{\cos^{16}\epsilon}{\cos^{16}\epsilon + \sin^{16}\epsilon}, \\ &\approx 1 - \epsilon^{16}. \end{aligned} \tag{24}$$

Now let us consider the case when an error is detected, say without loss of generality, on the first qubit of the eight qubit code. In this case, the fidelity is given by

$$\begin{aligned}&\mathscr{F}_{\text{error found}} = |{}_L\langle\phi|E_x^{\otimes 8}|\phi\rangle_L|^2 = \frac{|\alpha_1|^2}{\sum_{i=1}^{7}|\alpha_i|^2}, \\ &= \frac{\cos^{12}\epsilon}{\cos^{12}\epsilon + \cos^{10}\epsilon\sin^2\epsilon + \cos^8\epsilon\sin^4\epsilon + \cos^6\epsilon\sin^6\epsilon + \cos^4\epsilon\sin^8\epsilon + \cos^2\epsilon\sin^{10}\epsilon + \sin^{12}\epsilon}, \\ &\approx \frac{1}{1 + \epsilon^2 + \epsilon^4 + \epsilon^6 + \epsilon^8 + \epsilon^{10} + \epsilon^{12}}, \\ &\approx 1 - \epsilon^2 + O(\epsilon^4). \end{aligned} \tag{25}$$

From the above analysis using (23)–(25), it turned out that the fidelity of the output state using an encoded (logical) state (with or without detecting error) is always greater than the fidelity using an un-encoded (physical) state. More precisely, if no error is identified then the deviation from the original state is suppressed from $O(\epsilon^2)$ to $O(\epsilon^{16})$. In case of single error detection, the fidelity is at least the same as achieved by the physical state. Hence, in either case, the fidelity results achieved by encoded or logical state are better than that of the physical state.

Simulation results

In the following, we explain the capability of the suggested teleportation mechanism to effectively teleport an eight qubit physical state in a fault tolerant way. In this regard, we consider the following eight qubit physical state [38] and use Qiskit Aer Simulator with *qasm_simulator* as backend [39,40] to explain the proposed teleportation mechanism.

$$|\xi\rangle_{abcdefgh} = (\lambda|00000000\rangle + \mu|00100000\rangle + \nu|11011111\rangle + \omega|11111111\rangle)_{abcdefgh}, \tag{26}$$

where $|\lambda|^2 + |\mu|^2 + |\nu|^2 + |\omega|^2 = 1$. The quantum circuit to prepare this state and the obtained state are shown in Figs. 6 and 7, respectively.

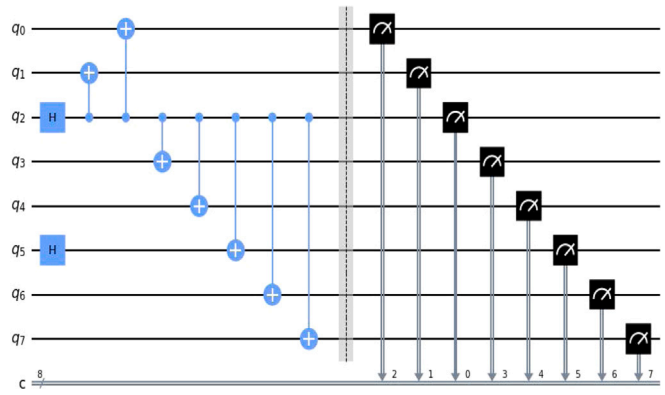

Fig. 6. The quantum circuit to prepare an unknown eight qubit state (26) where the coefficients $\lambda = \mu = \nu = \omega = \frac{1}{2}$.

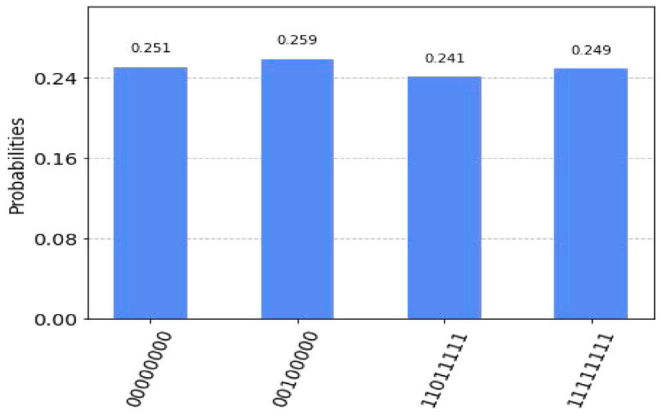

Fig. 7. The eight-qubit state possessed by Alice before teleportation.

In order to apply the proposed teleportation scheme, the eight-qubit state is locally deformed in a unitary fashion on Alice side as follows. Alice first applies swap gate on qubits with the indices b and c to obtain the state given by

$$|\xi\rangle_{acbdefgh} = (\lambda|00000000\rangle + \mu|01000000\rangle + \nu|10111111\rangle + \omega|11111111\rangle). \tag{27}$$

Subsequently, Alice performs CNOT operations on qubits with the indices d, e, f, g and h as the target qubits while qubit with index b as the control qubit. These operations yield the following eight qubit state

$$|\xi\rangle_{acbdefgh} = (\lambda|00000000\rangle + \mu|00100000\rangle + \nu|11000000\rangle + \omega|11100000\rangle)_{acbdefgh}. \tag{28}$$

The corresponding quantum circuit for these deformations is provided in Fig. 8. Note that by utilizing the above local unitary operations, on Alice side, we can obtain a relatively simple eight qubit state given by

$$|\xi\rangle_{acbdefgh} = (\lambda|000\rangle + \mu|001\rangle + \nu|110\rangle + \omega|111\rangle)_{acb} \otimes |00000\rangle_{defgh}. \tag{29}$$

It can be observed that the first three-qubit subsystem in the above mentioned eight-qubit state perfectly matches with the physical state (15). Hence, the state (29) can be teleported by utilizing the proposed teleportation mechanism 5 and the quantum channel (14) in a fault tolerant fashion. Finally, to recover the original eight qubit state (26), Bob performs the decoding process followed by CNOT and swap operations in the reverse order which Alice has applied on her side. The

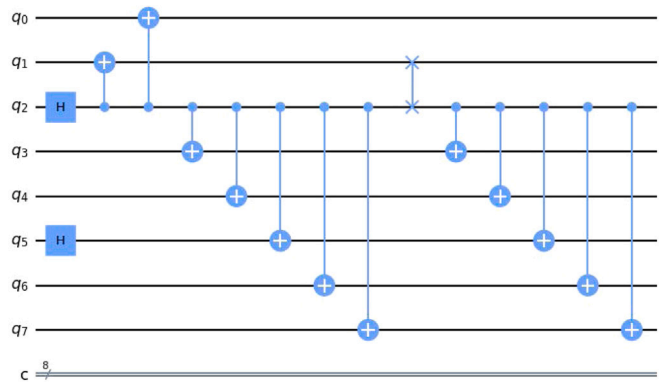

Fig. 8. The quantum circuit to prepare the eight-qubit state (28).

complete quantum circuit for the suggested teleportation mechanism and the teleported state (along with the ancillary qubits) are shown in Fig. 9.

Mathematically, the reconstructed state in Bob's possession is given by

$$|\chi\rangle = \sqrt{0.247}|00000000\rangle + \sqrt{0.247}|00100000\rangle + \sqrt{0.242}|11000000\rangle + \sqrt{0.264}|11111111\rangle. \tag{30}$$

It can be observed from Fig. 10 that the teleported state closely resembles with initial unknown state on Alice side with the fidelity of teleportation greater than 0.999.

The above example shows that the suggested teleportation mechanism has two fold advantages. Firstly, it can detect and correct one bit flip or phase flip error during teleportation by exploiting the inherent property of logical state entangled with the physical state in the quantum channel (14). Secondly, it may enhance resource efficient teleportation of multiqubit states using local unitary operations on either side without propagating errors since the logical operations, given by Table 1, involve transversal gates only.

Communication cost comparison

The cost of communication is also an important factor to evaluate the efficiency of a teleportation scheme. For this purpose we use and compare the transmission efficiency metric, κ, defined as [19]

$$\kappa = \frac{n_q}{n_{ch} + n_{cl} + n_{anc}}, \tag{31}$$

where n_q denotes the number of qubits to be teleported, n_{ch} denotes the number of channel particles, n_{cl} represents the number of classical bits transmitted and n_{anc} denotes the number of ancillary qubits.

In the following, we compare the transmission efficiency [19] of some of the recent multi-qubit teleportation schemes [19,41,42] with the proposed scheme. The comparison results are depicted in Table 6, where the larger value of κ indicates better transmission efficiency. In Refs. [41,42], four particles cluster is used as quantum channel to teleport three and two particle states, respectively, whereas the four particles entangled state is used to teleport seven qubit state in [19]. The present scheme used four qubit entangled state to teleport eight qubit state. It can be observed from Table 6 that the transmission efficiency of the proposed scheme is pretty much competitive with the rest of the schemes, yet not optimal. This seems reasonable due to an extra transmission overhead caused by logical nature of Bob's qubits. However, the transmission overhead can be justified owing to more reliable quantum teleportation using rigorous quantum error correction scheme and encoded qubits.

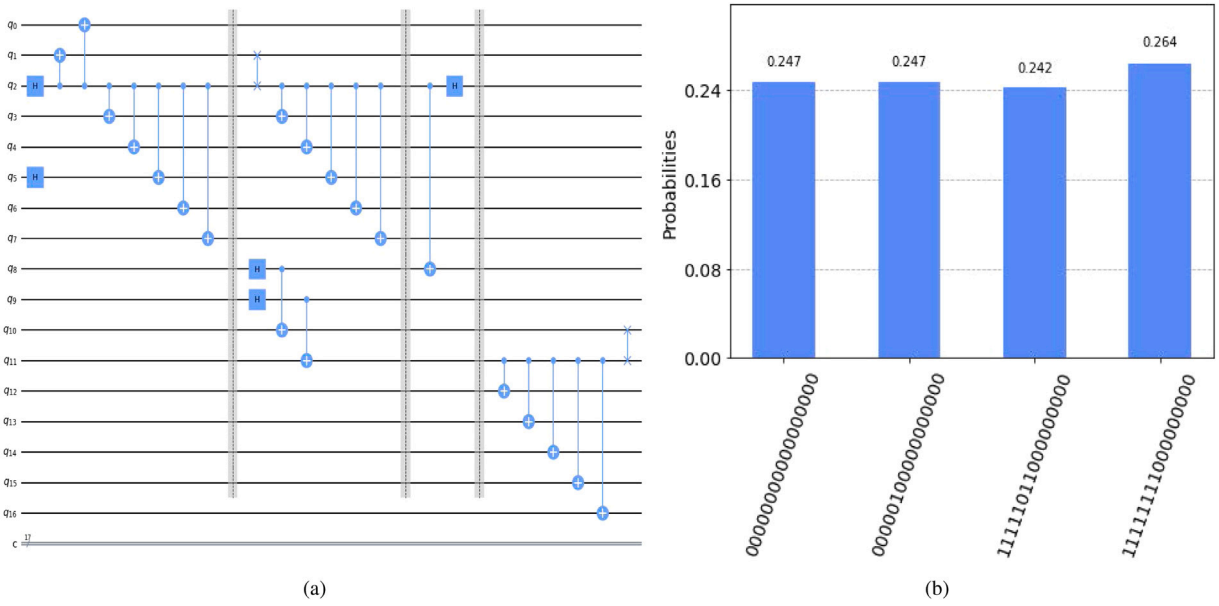

Fig. 9. The quantum circuit drawn in the left figure presents the complete teleportation mechanism. The right figure represents the teleported state.

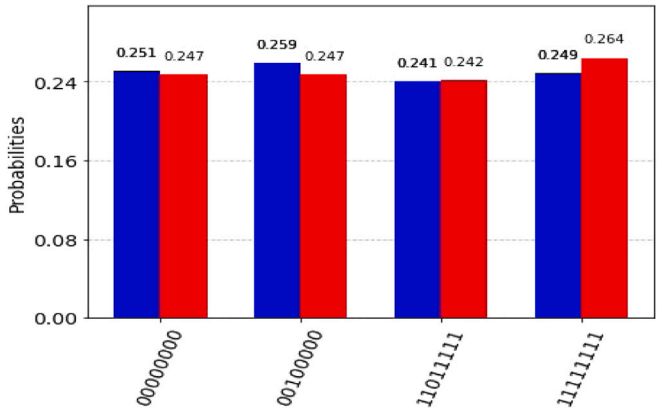

Fig. 10. The blue bars show the eight-qubit unknown quantum state on Alice side before teleportation. The red bars represent the teleported state on Bob side.

Table 6
Transmission efficiency comparison of multi-qubit teleportation schemes [19,41,42] with the proposed scheme.

Schemes	n_{ch}	n_q	$\kappa\%$
Ref. [41]	4	3	50%
Ref. [42]	4	2	25%
Ref. [19]	4	7	53.8%
Proposed scheme	4	8	44.4%

Security evaluation

Although the security analysis falls under the ambit of quantum cryptography, the teleportation methodology can somehow be scrutinized for certain security attacks. In the following, we briefly discuss two types of security problems namely, internal and external attacks.

Internal attack

In such type of attack, the receiver (Bob) is not trustworthy. That is, Bob either acts like Eve or Eve impersonates Bob while communicating with Alice. This situation leads to information leakage since Alice, oblivious of Bob's true identification, continues to send her measurement outcomes through the classical communication. This type of attack can be handled by introducing an additional authentication mechanism prior to commencing meaningful quantum communication. The authentication process can be designed with the help of quantum teleportation as follows [19].

Let us suppose that Alice and Bob share their respective identities (in the form of qubits) prior to starting any communication. Let the Bob's identity be represented by $|\psi\rangle_B = b_0|0\rangle_B + b_1|1\rangle_B$ and Bob wants to communicate with Alice. Further, assume that Alice and Bob have established a quantum channel using an entangled state. The authentication process starts with the joint Bell measurement of $|\psi\rangle_B$ with the qubit of the entangled pair on Bob's side. This action leads to the collapse of the entangled state along with the information of Bob's identity, $|\psi\rangle_B$, sent to Alice. Subsequently, Alice measures the qubit of the entangled pair on her side in accordance with the measurement outcome sent by Bob. This measurement enables Alice compare the communicated Bob's identity with the actual Bob's identity which was shared earlier. The successful comparison ascertains Bob's identity so that Alice can continue communication with Bob. Otherwise, Alice terminates the communication. It is important to note that even if Eve impersonates Bob, she has no access to the Bob's identification information which is known to Alice and Bob only. Hence, upon Alice measurement, the Bob's identity state sent by Eve will not match with $|\psi\rangle_B$.

External attack

The suggested mechanism is also examined for the external attack. For this purpose, a well known security attack is considered [19] where eavesdropper has secretly entangled an extra qubit with Bob's logical qubits without his knowledge, so that she can measure the extra particle to discover Bob's state. Without loss of generality, let us assume that Eve's qubit be of the form $|e\rangle = \frac{1}{\sqrt{2}}(|0\rangle + |1\rangle)_E$. In response to the suggested teleportation scheme, there are sixteen equi-probable collapsed states shared between Bob and Eve denoted by $|\psi^i\rangle_{234E} = |\overline{c_1c_2c_3}e\rangle$ which are given as follows

$$|\psi^1\rangle_{234E} = (\lambda|\overline{0000}\rangle + \lambda|\overline{0001}\rangle + \mu|\overline{0100}\rangle + \mu|\overline{0101}\rangle + \nu|\overline{1010}\rangle + \nu|\overline{1011}\rangle + \omega|\overline{1110}\rangle + \omega|\overline{1111}\rangle),$$

$$
\begin{aligned}
|\psi^2\rangle_{234E} &= (\lambda|\overline{0000}\rangle + \lambda|\overline{0001}\rangle - \mu|\overline{0100}\rangle - \mu|\overline{0101}\rangle \\
&\quad + \nu|\overline{1010}\rangle + \nu|\overline{1011}\rangle - \omega|\overline{1110}\rangle - \omega|\overline{1111}\rangle), \\
|\psi^3\rangle_{234E} &= (\lambda|\overline{0000}\rangle + \lambda|\overline{0001}\rangle + \mu|\overline{0100}\rangle + \mu|\overline{0101}\rangle \\
&\quad - \nu|\overline{1010}\rangle - \nu|\overline{1011}\rangle - \omega|\overline{1110}\rangle - \omega|\overline{1111}\rangle), \\
|\psi^4\rangle_{234E} &= (\lambda|\overline{0000}\rangle + \lambda|\overline{0001}\rangle - \mu|\overline{0100}\rangle - \mu|\overline{0101}\rangle \\
&\quad - \nu|\overline{1010}\rangle - \nu|\overline{1011}\rangle + \omega|\overline{1110}\rangle + \omega|\overline{1111}\rangle), \\
|\psi^5\rangle_{234E} &= (\lambda|\overline{0100}\rangle + \lambda|\overline{0101}\rangle + \mu|\overline{0000}\rangle + \mu|\overline{0001}\rangle \\
&\quad + \nu|\overline{1110}\rangle + \nu|\overline{1111}\rangle + \omega|\overline{1010}\rangle + \omega|\overline{1011}\rangle), \\
|\psi^6\rangle_{234E} &= (\lambda|\overline{0100}\rangle + \lambda|\overline{0101}\rangle - \mu|\overline{0000}\rangle - \mu|\overline{0001}\rangle \\
&\quad + \nu|\overline{1110}\rangle + \nu|\overline{1111}\rangle - \omega|\overline{1010}\rangle - \omega|\overline{1011}\rangle), \\
|\psi^7\rangle_{234E} &= (\lambda|\overline{0100}\rangle + \lambda|\overline{0101}\rangle + \mu|\overline{0000}\rangle + \mu|\overline{0001}\rangle \\
&\quad - \nu|\overline{1110}\rangle - \nu|\overline{1111}\rangle - \omega|\overline{1010}\rangle - \omega|\overline{1011}\rangle), \\
|\psi^8\rangle_{234E} &= (\lambda|\overline{0100}\rangle + \lambda|\overline{0101}\rangle - \mu|\overline{0000}\rangle - \mu|\overline{0001}\rangle \\
&\quad - \nu|\overline{1110}\rangle - \nu|\overline{1111}\rangle + \omega|\overline{1010}\rangle + \omega|\overline{1011}\rangle), \\
|\psi^9\rangle_{234E} &= (\lambda|\overline{1010}\rangle + \lambda|\overline{1011}\rangle + \mu|\overline{1110}\rangle + \mu|\overline{1111}\rangle \\
&\quad + \nu|\overline{0000}\rangle + \nu|\overline{0001}\rangle + \omega|\overline{0100}\rangle + \omega|\overline{0101}\rangle), \\
|\psi^{10}\rangle_{234E} &= (\lambda|\overline{1010}\rangle + \lambda|\overline{1011}\rangle - \mu|\overline{1110}\rangle - \mu|\overline{1111}\rangle \\
&\quad + \nu|\overline{0000}\rangle + \nu|\overline{0001}\rangle - \omega|\overline{0100}\rangle - \omega|\overline{0101}\rangle), \\
|\psi^{11}\rangle_{234E} &= (\lambda|\overline{1010}\rangle + \lambda|\overline{1011}\rangle + \mu|\overline{1110}\rangle + \mu|\overline{1111}\rangle \\
&\quad - \nu|\overline{0000}\rangle - \nu|\overline{0001}\rangle - \omega|\overline{0100}\rangle - \omega|\overline{0101}\rangle), \\
|\psi^{12}\rangle_{234E} &= (\lambda|\overline{1010}\rangle + \lambda|\overline{1011}\rangle - \mu|\overline{1110}\rangle - \mu|\overline{1111}\rangle \\
&\quad - \nu|\overline{0000}\rangle - \nu|\overline{0001}\rangle + \omega|\overline{0100}\rangle + \omega|\overline{0101}\rangle), \\
|\psi^{13}\rangle_{234E} &= (\lambda|\overline{1110}\rangle + \lambda|\overline{1111}\rangle + \mu|\overline{1010}\rangle + \mu|\overline{1011}\rangle \\
&\quad + \nu|\overline{0100}\rangle + \nu|\overline{0101}\rangle + \omega|\overline{0000}\rangle + \omega|\overline{0001}\rangle), \\
|\psi^{14}\rangle_{234E} &= (\lambda|\overline{1110}\rangle + \lambda|\overline{1111}\rangle - \mu|\overline{1010}\rangle - \mu|\overline{1011}\rangle \\
&\quad + \nu|\overline{0100}\rangle + \nu|\overline{0101}\rangle - \omega|\overline{0000}\rangle - \omega|\overline{0001}\rangle), \\
|\psi^{15}\rangle_{234E} &= (\lambda|\overline{1110}\rangle + \lambda|\overline{1111}\rangle + \mu|\overline{1010}\rangle + \mu|\overline{1011}\rangle \\
&\quad - \nu|\overline{0100}\rangle - \nu|\overline{0101}\rangle - \omega|\overline{0000}\rangle - \omega|\overline{0001}\rangle), \\
|\psi^{16}\rangle_{234E} &= (\lambda|\overline{1110}\rangle + \lambda|\overline{1111}\rangle - \mu|\overline{1010}\rangle - \mu|\overline{1011}\rangle \\
&\quad - \nu|\overline{0100}\rangle - \nu|\overline{0101}\rangle + \omega|\overline{0000}\rangle + \omega|\overline{0001}\rangle). \qquad (32)
\end{aligned}
$$

Note that Bob's qubits $\overline{c_1c_2c_3}$ are logical or encoded states. It can be observed that the suggested mechanism offers security against such attacks in two ways. Firstly, the collapsed state $|\psi^i\rangle_{234E}$ is separable. For instance $|\psi^1\rangle_{234E}$ can be expressed as a direct product

$$
|\psi^1\rangle_{234E} = (\lambda|\overline{000}\rangle + \mu|\overline{010}\rangle + \nu|\overline{101}\rangle + \omega|\overline{111}\rangle)_{234} \otimes (|0\rangle + |1\rangle)_E. \qquad (33)
$$

Hence, Eve can seek nothing about the teleported state. Secondly, the teleported state owned by Bob is not physical rather it is the encoded state. Thus, Eve does not have any information whether the qubits owned by Bob are physical or logical states and which type of encoding scheme is employed by Bob.

Conclusion

We suggested an innovative quantum teleportation mechanism where a multi-qubit physical state is teleported into another multi-qubit but logical state. The suggested mechanism significantly differs from the conventional teleportation which teleports a physical qubit on sender's side into a physical qubit on the receiver's side. The proposed scheme is substantiated by the teleportation of an eight-qubit physical state via a four-qubit state where the receiver possesses three logical qubits. The advantages of the proposed mechanism are threefold. Firstly, the rigorous logical encoding framework enables the suggested strategy detection and correct the most common bit and phase error on any one of the multi-qubit state. Secondly, the transversal nature of logical operations on the encoded qubits not only offers resistance to error detection but also prevents the propagation of errors through the quantum circuits. Thirdly, the suggested mechanism is resource efficient since it facilitates multi-qubit teleportation using fewer resources. Owing to these distinguished features, the proposed teleportation scheme may have significant contributions towards the near future fault tolerant computing.

Declaration of competing interest

The authors declare that they have no known competing financial interests or personal relationships that could have appeared to influence the work reported in this paper.

Data availability

Data will be made available on request.

Acknowledgments

Asif Mushtaq would like to thank Mathematics Teaching and Learning, research group within the Department of Mathematics, Bodø, Nord University, Norway for the partial support. Zahid Hussain Shamsi would like to thank the Department of Mathematics, University of the Punjab, Pakistan for the partial support.

References

[1] Ren J-G, Xu P, Yong H-L, Zhang L, Liao S-K, Yin J, et al. Ground-to-satellite quantum teleportation. Nature 2017;549(7670):70–3. http://dx.doi.org/10.1038/nature23675.

[2] Bennett CH, Brassard G, Crépeau C, Jozsa R, Peres A, Wootters WK. Teleporting an unknown quantum state via dual classical and Einstein-Podolsky-Rosen channels. Phys Rev Lett 1993;70(13):1895.

[3] Einstein A, Podolsky B, Rosen N. Can quantum-mechanical description of physical reality be considered complete? Phys Rev 1935;47:777–80. http://dx.doi.org/10.1103/PhysRev.47.777, URL https://link.aps.org/doi/10.1103/PhysRev.47.777.

[4] Bouwmeester D, Pan J-W, Mattle K, Eibl M, Weinfurter H, Zeilinger A. Experimental quantum teleportation. Nature 1997;390(6660):575–9. http://dx.doi.org/10.1038/37539.

[5] Boschi D, Branca S, De Martini F, Hardy L, Popescu S. Experimental realization of teleporting an unknown pure quantum state via dual classical and Einstein-Podolsky-Rosen channels. Phys Rev Lett 1998;80:1121–5. http://dx.doi.org/10.1103/PhysRevLett.80.1121, URL https://link.aps.org/doi/10.1103/PhysRevLett.80.1121.

[6] Riebe M, Chwalla M, Benhelm J, Häffner H, Hänsel W, Roos C, et al. Quantum teleportation with atoms: quantum process tomography. New J Phys 2007;9(7):211.

[7] Nölleke C, Neuzner A, Reiserer A, Hahn C, Rempe G, Ritter S. Efficient teleportation between remote single-atom quantum memories. Phys Rev Lett 2013;110(14):140403.

[8] Kim Y-H, Kulik SP, Shih Y. Quantum teleportation of a polarization state with a complete bell state measurement. Phys Rev Lett 2001;86:1370–3. http://dx.doi.org/10.1103/PhysRevLett.86.1370, URL https://link.aps.org/doi/10.1103/PhysRevLett.86.1370.

[9] Wang X-L, Cai X-D, Su Z-E, Chen M-C, Wu D, Li L, et al. Quantum teleportation of multiple degrees of freedom of a single photon. Nature 2015;518(7540):516–9.

[10] Sun Y-H, Xie Y-X. Memory effect of a dephasing channel on measurement uncertainty, dense coding, teleportation, and quantum Fisher information. Results Phys 2022;37:105526. http://dx.doi.org/10.1016/j.rinp.2022.105526, URL https://www.sciencedirect.com/science/article/pii/S2211379722002637.

[11] Zubarev A, Cuzminschi M, Isar A. Continuous variable quantum teleportation of a thermal state in a thermal environment. Results Phys 2022;39:105700. http://dx.doi.org/10.1016/j.rinp.2022.105700, URL https://www.sciencedirect.com/science/article/pii/S2211379722003837.

[12] Pirandola S, Eisert J, Weedbrook C, Furusawa A, Braunstein SL. Advances in quantum teleportation. Nat Photonics 2015;9(10):641–52. http://dx.doi.org/10.1038/nphoton.2015.154.

[13] Li C, Song H-S, Luo Y-X. Criterion for general quantum teleportation. Phys Lett A 2002;297(3–4):121–5.

[14] Bae J, Jin J, Kim J, Yoon C, Kwon Y. Three-party quantum teleportation with asymmetric states. Chaos Solitons Fractals 2005;24(4):1047–52.

[15] Shi-Biao Z. Teleportation of quantum states through mixed entangled pairs. Chin Phys Lett 2006;23(9):2356.

[16] Shao Q. Quantum teleportation of the two-qubit entangled state by use of four-qubit entangled state. Internat J Theoret Phys 2013;52:2573–7.

[17] Li Y-h, Sang M-h, Wang X-p, Nie Y-y. Quantum teleportation of a four-qubit state by using six-qubit cluster state. Internat J Theoret Phys 2016;55:3547–50.
[18] Yang G, Lian B-W, Nie M, Jin J. Bidirectional multi-qubit quantum teleportation in noisy channel aided with weak measurement. Chin Phys B 2017;26(4):040305.
[19] Zheng Y, Li D, Liu X, Liu M, Zhou J, Yang X, et al. Quantum teleportation of unknown seven-qubit entangled state using four-qubit entangled state. Internat J Theoret Phys 2022;61(5):133.
[20] Zhou R-G, Li X, Qian C, Ian H. Quantum bidirectional teleportation 2? 2 or 2? 3 qubit teleportation protocol via 6-qubit entangled state. Internat J Theoret Phys 2020;59:166–72.
[21] Zhou R-G, Qian C, Ian H. Bidirectional quantum teleportation of two-qubit state via four-qubit cluster state. Internat J Theoret Phys 2019;58:150–6.
[22] Sadeghi-Zadeh MS, Houshmand M, Aghababa H, Kochakzadeh MH, Zarmehi F. Bidirectional quantum teleportation of an arbitrary number of qubits over noisy channel. Quantum Inf Process 2019;18:1–19.
[23] Li D, Zheng Y, Liu X, Liu M. Hierarchical quantum teleportation of arbitrary single-qubit state by using four-qubit cluster state. Internat J Theoret Phys 2021;60:1911–9.
[24] Xu G, Wang C, Yang Y-X. Hierarchical quantum information splitting of an arbitrary two-qubit state via the cluster state. Quantum Inf Process 2014;13:43–57.
[25] Wang X-W, Zhang D-Y, Tang S-Q, Xie L-J. Multiparty hierarchical quantum-information splitting. J Phys B: At Mol Opt Phys 2011;44(3):035505.
[26] Bai M-Q, Mo Z-W. Hierarchical quantum information splitting with eight-qubit cluster states. Quantum Inf Process 2013;12:1053–64.
[27] Rajiuddin S, Baishya A, Behera BK, Panigrahi PK. Experimental realization of quantum teleportation of an arbitrary two-qubit state using a four-qubit cluster state. Quantum Inf Process 2020;19:1–13.
[28] Kumar A, Haddadi S, Pourkarimi MR, Behera BK, Panigrahi PK. Experimental realization of controlled quantum teleportation of arbitrary qubit states via cluster states. Sci Rep 2020;10(1):13608.
[29] Devitt SJ, Munro WJ, Nemoto K. Quantum error correction for beginners. Rep Progr Phys 2013;76(7):076001. http://dx.doi.org/10.1088/0034-4885/76/7/076001.
[30] Calderbank AR, Rains EM, Shor PW, Sloane NJA. Quantum error correction and orthogonal geometry. Phys Rev Lett 1997;78:405–8. http://dx.doi.org/10.1103/PhysRevLett.78.405, URL https://link.aps.org/doi/10.1103/PhysRevLett.78.405.
[31] Gottesman D. Stabilizer codes and quantum error correction. 1997, http://dx.doi.org/10.48550/ARXIV.QUANT-PH/9705052, arXiv, URL https://arxiv.org/abs/quant-ph/9705052.
[32] Gottesman D. Class of quantum error-correcting codes saturating the quantum hamming bound. Phys Rev A 1996;54:1862–8. http://dx.doi.org/10.1103/PhysRevA.54.1862, URL https://link.aps.org/doi/10.1103/PhysRevA.54.1862.
[33] Preskill J. Lecture notes for ph219/cs219: Quantum information and computation. 2001, URL http://theory.caltech.edu/~preskill/ph229.
[34] Valivarthi R, Davis SI, Peña C, Xie S, Lauk N, Narváez L, et al. Teleportation systems toward a quantum internet. PRX Quantum 2020;1:020317. http://dx.doi.org/10.1103/PRXQuantum.1.020317, URL https://link.aps.org/doi/10.1103/PRXQuantum.1.020317.
[35] Laflamme R, Miquel C, Paz JP, Zurek WH. Perfect quantum error correcting code. Phys Rev Lett 1996;77:198–201. http://dx.doi.org/10.1103/PhysRevLett.77.198, URL https://link.aps.org/doi/10.1103/PhysRevLett.77.198.
[36] Luo Y-H, Chen M-C, Erhard M, Zhong H-S, Wu D, Tang H-Y, et al. Quantum teleportation of physical qubits into logical code spaces. Proc Natl Acad Sci 2021;118(36):e2026250118. http://dx.doi.org/10.1073/pnas.2026250118, URL https://www.pnas.org/doi/abs/10.1073/pnas.2026250118.
[37] Nielsen MA, Chuang IL. Quantum computation and quantum information. Cambridge University Press; 2010.
[38] Zhao N, Li M, Chen N, Zhu C-h, Pei C-x. Quantum teleportation of eight-qubit state via six-qubit cluster state. Internat J Theoret Phys 2018;57:516–22.
[39] Abraham H, et al. Qiskit: An open-source framework for quantum computing. 2021, http://dx.doi.org/10.5281/zenodo.2573505.
[40] IBM Quantum, https://quantum-computing.ibm.com.
[41] Li Y-h, Li X-l, Nie L-p, Sang M-h. Quantum teleportation of three and four-qubit state using multi-qubit cluster states. Internat J Theoret Phys 2016;55:1820–3.
[42] Liu Z-m, Zhou L. Quantum teleportation of a three-qubit state using a five-qubit cluster state. Internat J Theoret Phys 2014;53:4079–82.